International Journal of Engineering, Management & Technology (IJEMT)
www.ijemt.com, Volume 3 Issue I, May 2024, PP 19 - 29, ISSN (Online): 2583 – 4517

Exploring Particle Yields in Heavy-Ion Collisions: Investigating Resonances and Hadronic Interactions with the Statistical Hadronization Model

Deekshit Kumar[*1], Yajvendra Kumar[2], Chandrawati[3], P.K Tyagi[4]
[1,2,3,4]DPBS College, Anupshahr, Bulandshahr, U.P India - 203390

Abstract: *Heavy-ion collisions at high energies create extreme conditions akin to those found in the early cosmos. Understanding the transition from quarks and gluons to hadrons and unraveling the characteristics of nuclear matter demands a comprehensive analysis of particle creation in such scenarios. In this paper, we leverage the Statistical Hadronization Model (SHM) to scrutinize the impact of resonances and hadronic interactions on particle yields in heavy-ion collisions. The SHM provides a robust framework for characterizing particle creation, integrating statistical mechanics principles with the properties of known resonances to forecast particle yields. By considering the available phase space and the probabilities of various hadronic interactions, the SHM facilitates a deeper comprehension of the particle composition observed in experiments. Our study conducts a meticulous examination of particle yields across a spectrum of heavy-ion collision scenarios, encompassing diverse collision energies and system sizes. Through a comparative analysis with experimental data, we elucidate the role of resonances and hadronic interactions in shaping the final particle spectra. Our findings underscore the substantial influence of resonances on particle production, particularly evident in the contribution of decay products, especially for particles with higher masses. Furthermore, we observe deviations from complete thermalization due to the influence of hadronic interactions on particle yields. These insights contribute significantly to our understanding of the fundamental mechanisms governing particle creation in heavy-ion collisions, advancing our knowledge of nuclear matter under extreme conditions and refining the statistical hadronization model. Our study underscores the imperative for the SHM to account for both resonances and hadronic interactions to accurately predict particle yields in heavy-ion collisions. Continued advancements in modeling will further illuminate the dynamics of the early cosmos and the quark-gluon plasma, fostering deeper insights into these fundamental phenomena.*

Keywords: *Heavy-ion collisions, Particle yields, Resonances, Hadronic interactions, Statistical Hadronization Model (SHM)*

INTRODUCTION

Resonance generation is a crucial aspect of both heavy and elementary ion collisions since it may occur concurrently in each of these processes. The finding that a significant fraction of the particles in the final state are resonance decay products has enhanced our understanding of the mechanism by which hadrons are generated in pp and $e+e^-$ collisions. [1-4]

Short-lived resonances like (1020), (1520), (1385), and (1530)0, as well as K*(892)0 and (770), offer valuable insights into the dynamics of hadron chemistry and strangeness generation in heavy-ion collisions. These resonances are observable in collisions of heavy ions. The (1020) resonance, in particular, possesses a peculiar property that remains unexplained. Our understanding of the various processes contributing to the formation of particle spectra at low-to-intermediate transverse momenta (p_T) is further enriched by investigating the baryon-to-meson ratios of

[*] **Manuscript Received on: May 12, 2024**
Manuscript Published on www.ijemt.com : May 17, 2024
Corresponding Author: Deekshit Kumar

particles with comparable masses, such as p/(1020) and p/K*(892)0. Resonances also provide a means to study crucial characteristics of the hadronic phase, including density and lifetime. [5-7]

Hadronic Phase

The yields of long-lived particles are predicted to remain unchanged after chemical freeze out, despite the fact that scattering mechanisms are predicted to continue to affect resonance yields throughout the hadronic phase and up until kinetic freeze out. Despite the fact that following chemical freeze out, it is anticipated that the yields of long-lived particles would not vary, this forecast is made. Despite the fact that it was anticipated there would be no change in the yields of long-lived particles after chemical freeze out, this is the case. As an illustration, one method that may be used to renew resonance yields is hadron pseudoelastic scattering. This is certainly conceivable. The decay products of resonances that decay during the hadronic phase could potentially be subjected to elastic collisions, which could make it more challenging to reconstruct the resonance, or pseudoelastic scattering through a new resonance state, which would hide information about the original resonance. [8-12]

Resonance peak extraction from the collected invariant mass distributions:

The resonances are abundantly created in hadronic and heavy-ion collisions, and they may be easily and simply seen experimentally in the main hadronic decay channels. Heavy ions are another component that helps to create the resonances. Due to the mass difference between the father and daughter particles, the resonance measurements' momentum range can go all the way down to zero momenta. The cause of this is the difference in masses between the father and daughter particles. This mass disparity genuinely causes the momenta of the daughter particle to increase. Even if it were difficult to locate charged hadrons with low momentum, on the scale of a few hundred MeV/c or less, this claim would still hold true.[13-16]

At higher moments, when the particle multiplicities and, consequently, the combinatorial background, are fairly low, it is considerably harder to find hadrons using a variety of techniques. As a direct consequence of this, it can now distinguish between the resonance peaks and the estimated invariant mass distributions. Despite the high multiplicity, resonances spanning a large range of transverse momentum (p_T) may still be empirically identified in the setting of core heavy-ion collisions. Despite the fact that it can seem nonsensical, this is the case. Due to the interaction of all of these elements, this is now possible. The experimental setup must be able to provide a high efficiency of track reconstruction in a broad acceptance with a momentum resolution of less than 1% and identification of the charged hadrons in the final state for the measurements to be successful. [17-19]

Models based on heavy ion collisions using ad hoc parameters:

On the basis of the use of statistical research approaches, Hagedorn has also theorized the existence of elementary processes that produce particles, such as $e^+ + e^-$ processes and $p^+ p^-$ processes. Recent studies have demonstrated that there is a significant match for yields and even transverse-momentum spectra observed in basic processes using the same model that correctly describes hadron yields in HIC. A thorough inquiry led to the discovery of this. As a direct result of the fact that both models use the exact same data, this result was made achievable. The main component that enabled the finding of this conclusion possible was the model's capacity to precisely measure hadron yields in HIC. [20-23] The conclusions about chemical equilibrium in heavy ion collisions drawn from comparing the data to the hadron yields predicted by statistical model simulations are called into question by these findings, and they offer a more fundamental explanation for the consistency of the two sets of observations. These conclusions were reached by comparing the data to the hadron yields anticipated by simulations of statistical models. To put it another way, these results raise questions about the generalizations made about the chemical equilibrium that takes place in collisions involving heavy ions.

Ad hoc parameterized models are more likely to deviate from equilibrium since different realizations may handle the variables differently. Models with these traits frequently make these distinctions. In order to further suppress particles that incorporate strangeness, the authors of use a mixed canonical ensemble, retaining strangeness precisely

as well as an extra multiplicative component s. This is carried out in order to further reduce particles that contain strangeness. The grand canonical ensemble, in contrast, only accounts for the factors T (temperature), B (baryochemical potential), and V (system volume). The grand canonical ensemble, however, only makes use of these three parameters to simulate core heavy-ion collisions. This is so because the huge canonical ensemble is built on the foundation of the standard model. On the other hand, because it needs s in addition to an additional parameter known as q, the synthesis of the light quarks u and d is impossible in in. This stops the synthesis from taking place. To do this, the manufacturing of light quarks must be stopped.[24-26] The authors of also employ a mixed canonical ensemble, but they substitute V_c (or R_c) for s as the strangeness correlation volume parameter. The sole difference between V_c and s is the projected meson yield, which is also the only factor that matters. That yield is the only factor that counts. There is no drop in the yield of when the V_c formalism is used, but there is a significant reduction in the yield when the s formalism is used. The reason for this is that the state in question is a "ss state," which is one that by definition retains its strangeness. It is known how these non-equilibrium characteristics affect the degree of centralization of the system as well as the importance of the system as a whole. The authors' fascinating finding is that the strangeness suppression factor dramatically increases as the system's scale rises.[27]

OBJECTIVES OF THE STUDY

1. To study identification of hadrons with different techniques and the particle multiplicities.
2. To study on Heavy ion collisions-based Models with Ad Hoc Parameters

RESEARCH METHODOLOGY

Throughout the entirety of the process of gathering the pp data, a trigger with a slight amount of bias, represented by the letter MB, was utilized. In order for the logic to work properly, the MB trigger needs a hit in either the V0A or the V0C detector at the same time as the LHC bunch crossover in addition to a hit in the SPD detector in the middle barrel. One of the criteria that is utilized throughout the process of preventing pileup in pp collisions is one that is based on the offline reconstruction of a number of significant vertices in the SPD. This particular criterion is utilized as part of the procedure. In order to avoid a buildup of particles, it is necessary to employ this criterion during the evaluation process. This is done in order to prevent pileups, which are an undesirable consequence that must be avoided at all costs and can only be prevented by doing this. [28-31]A pileup occurs when many encounters occur concurrently at a single group crossing. It is estimated that fewer than one percent of all incidents are considered to be rejected pileups; as a result, this group only accounts for a negligible portion of all accidents. In addition, an MB trigger was utilized in order to accumulate Pb-Pb data. This trigger makes use of logic that requires synchronous signal occurrences in both V0A and V0C in order for it to be triggered. This is a requirement for activation. The MB-initiated collisions are analyzed in both the pp and the Pb-Pb collisions to determine if the reconstructed position of the collision vertex along the beam axis (V_z, zis the longitudinal direction) is within 10 cm of the nominal interaction point. In order to identify whether or whether the MB was the source of the occurrence that took happened, this must take place. This analysis won't be carried out until a reconstructed collision vertex can be found for the occurrences. The timing information provided by the Zero Degree Calorimeters (ZDC_s) and the V0 detectors is utilized in order to filter out and reject any potential background events that may take place. In order to obtain the most accurate results possible from the Pb-Pb research, all eight of the different forms of centrality that are now known are utilized. [32-34]

In the classes 0–10% and 70–80%, respectively, Pb-Pb collisions with impact parameters that are low and high, respectively, occur most often and peripherally. After the requirements for event selection have been met, there will be an examination of 110 million pp events as well as 30 million Pb-Pb collisions. In a manner comparable to that of past research, charged recordings are selected for examination on the basis of track selection criteria that ensure an exceptionally high level of track quality. Each track in the TPC needs to have at least 70 crossing rows and no more than 159 horizontal segments in the transverse readout plane.[35] The maximum number of horizontal segments is

159. There is a limit of 159 horizontal segments that can be present. These settings are absolutely ideal for each individual piece of music.[36-38] A p_T-dependent selection criterion on the distance of closest approach to the collision vertex in the transverse (xy) plane and in the longitudinal direction (DCA_z) is applied in order to lessen the amount of pollution caused by secondary charged particles that originate from weakly decaying hadrons. This is done in the transverse (xy) plane and in the longitudinal direction (DCA_z). This is accomplished in both the transverse plane (xy) and the longitudinal direction (DCA_z). In order to do this, we make use of the transverse plane (xy) in addition to the longitudinal direction (DCAz). In order for tracks to be taken into consideration, they need to fulfill the following selection conditions in addition to having a p_T that is more than 0.15 GeV/c in both pp and Pb-Pb collisions. It is generally agreed upon that charged particles with pseudorapidities ranging from 0.8 to 0.9 may be safely worked with.[39]

Corrections, normalization, and yield extraction:

The first stage in recreating the K*0 and 0 resonances is to determine the invariant mass of the resonances' decay products, which occur through hadronic decay channels.

. $K^{*0}(\overline{K}^{*0}) \rightarrow K^{+}\pi^{-}(K^{-}\pi^{+})$ (Branching Ratio, BR = 66.666 ±0.006%) and φ→K*+K*0⁻(BR = 49.2 ±0.5%), Particles with oppositely charged K^+ and (or K^-) that are emitted from the same event are joined together in order to generate the invariant mass distributions of K^0. The K^* and K^*K^{*0} pairs are chosen as candidates for selection within the quickness range. |y|<0.5 when both pp collisions and Pb-Pb collisions take place at the same time. Because of the uncorrelated mass components, it has been proved that the invariant mass distribution has both a signal peak and a sizeable combinatorial background. This is due to the fact that the mass components do not correlate with one another. K^* pairings, often commonly referred to as K^*K^{*0} pairs. In order to conduct an accurate analysis of the combinatorial background present in each of the collision systems, a mixed-event approach is utilized. In order to produce the mixed-event backdrop, the kaons that were not used during one event are merged with those that were used during another event that had the opposite charge. (K) is selected from a group consisting of unique implementations of the K^0 function. In order to produce results that can be relied upon, it is absolutely necessary for the combined events to share features that are analogous to those of one another. In order for the Pb-Pb technique to successfully combine the two events, they need to come from the same centrality class, and the positions of their collision vertex value 1. $|\Delta V_z|$ < The mixing of two events and a condition of within 1 cm are included in pp collisions.[40] $|\Delta V_z|$ < 1 centimeter, as well as a shift in the density of electrically charged particles despite rapid movement.

$(|\Delta y| < 0.5)$ number less than five in total. In order to mitigate the impact that random statistical fluctuations\might have on the background distribution, each event is consolidated with five extra occurrences. When the invariant mass distribution from the mixed event is measured in the mass region of 1.1-1.3 (or 1.04-1.06) GeV/c^2 for K*^{0}(or), which is some distance from the mass peak, it is normalized to the distribution of oppositely charged couples for the same event. This occurs when the invariant mass distribution is measured in the mass region of 1.1-1.3 (or 1.04-1.06) GeV/$c^2$for K*^{0}(or). (for K^{*0}) $7\Gamma$for φ, Γ may be conceptualized as the extent to which the resonance is felt). Following the combinatorial reduction of the background, the signal peak may be observed superimposed over the remnants of the background. [41-43]

DATA ANALYSIS

Systematic uncertainties:

The systematic errors discovered during the estimation of the K^0 and yields for pp and Pb-Pb collisions are listed in Table 1. These errors were discovered throughout the estimating process. [44-46]The principal causes of systematic errors are the yield extraction method, the PID and track selection criteria, the global tracking efficiency, the knowledge of the ALICE material budget, and the comprehension of the interaction cross section of hadrons in the

detector material. It is demonstrated that the transverse momentum can have three different values: low, medium, and high p_T, together with the corresponding levels of uncertainty for each value. The numbers in the table represent the average of all the centralities for Pb-Pb collisions, and all classes of centrality, with the exception of the one associated with yield extraction, have the same systematic uncertainties. [47]The technique used to determine yield takes into account the uncertainties brought on by variations in the fitting range, the methodology chosen for the combinatorial background estimate, the normalizing range, and the residual background's shape. According to calculations, the yield extraction uncertainties for K^0 in pp vary from 7.9-11.8% (corresponding to 2.4-3.5% for the), and for Pb-Pb collisions, they range from 7.3-10.1% (corresponding to 1.9-4.9%). For your convenience, the percentages for each range are displayed below. Between 2.1 and 6.9% (or 0.3 and 6.5%, respectively) are the PID systematic uncertainties for K^0 in pp and Pb-Pb collisions, with the former number being higher. By comparing the data for single charged particles, one may determine how much the global tracking efficiency has contributed to the uncertainty. Combining the two charged tracks utilized in the invariant mass reconstruction of K^0 and results in an uncertainty range of 2.0-8.2%. The percentage of the total that is changeable as a result of the track selection criterion is between 1.0 and 5.5%. The systematic errors caused by the hadronic interaction cross section are expected to make up less than 2.8% of the total and only become significant at low p_T (less than 2 GeV/c).

Table 1: Systematic errors in K^{*0} and Yield measurements for collisions between pp and pb $\sqrt{s_{NN}} = 5.02$ TeV. These ambiguities are presented for three distinct values of transverse momentum: low, medium, and high p_T respectively. All of the systematic uncertainties, with the exception of the yield extraction, are shared by the different centrality classes for Pb–Pb collisions. The values that are provided in the table are an average of those that are shared by all of the centrality classes.

Systematic variation	Pb–Pb					pp						
	K^{*0}			φ		K^{*0}			φ			
	p_T(GeV/c)			p_T(GeV/c)		p_T(GeV/c)			p_T(GeV/c)			
	0.1	4.5	17	0.4	4.24	17	0.2	4.24	17	0.5	4.24	17
Yield extraction (%)	7.2	7.1	10.0	4.3	1.7	4.2	11.6	7.7	8.1	2.3	3.4	3.4
Track selection (%)	2.8	1.3	3.1	3.1	1.2	1.1	1.3	1.1	1.8	4.1	2.1	5.4
Particle identification (%)	5.3	3.1	5.1	1.1	1.4	2.3	2.2	3.1	6.8	0.2	1.6	6.4
Global tracking efficiency (%	4.3	7.2	4.1	4.3	8.1	3.2	2.1	3.3	3.5	2.1	3.1	2.3
Material budget (%)	1.3	0	0	5.4	0	0	3.3	0	0	5.1	0	0
Hadronic Interaction (%)	2.4	0	0	1.3	0	0	2.8	0	0	1.2	0	0
Total (%	10.7	11.1	12.1	9.2	8.5	6.4	13.1	9.3	11.6	7.8	5.3	9.4

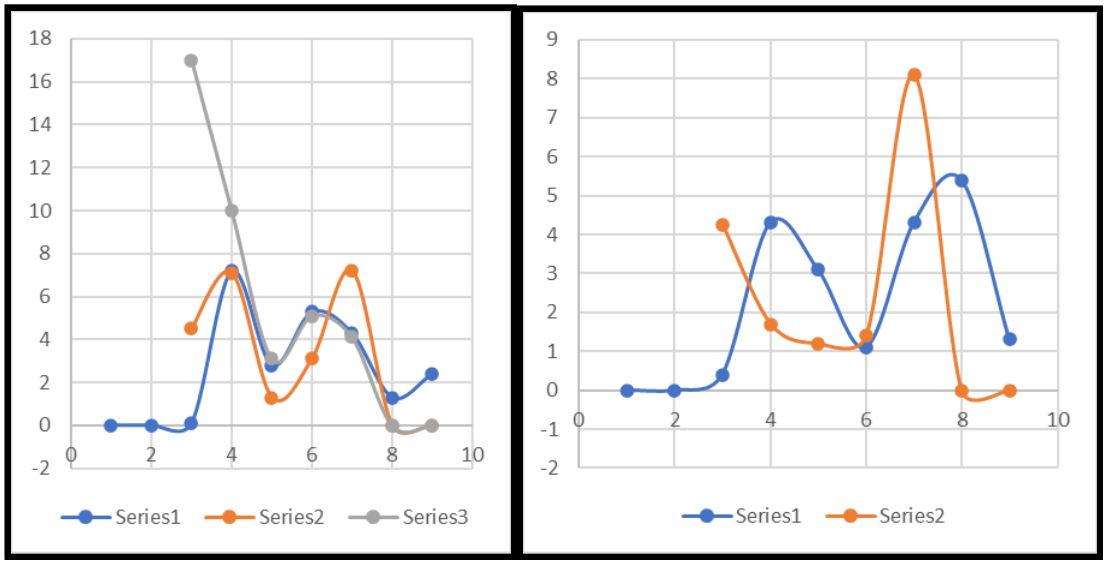

Fig. 1. The distributions of the several centrality classes in Pb-Pb collisions at different energies, as well as the p_T distributions of (a) K^{*0} and (b) mesons in pp collisions, are presented below. $\sqrt{s_{NN}} = 5.02$ TeV. The data may be shown for analysis by being plotted in the middle of each bin. The bars and boxes in this graph, respectively, indicate the systematic and statistical uncertainty.

collisions between pp and Pb-Pb, as well as the transverse momentum spectrum corresponding to these events The $p_T$distributions of the K^{*0} and mesons are shown in Figure 1 for the value of |y| 0.5. The efficiency, acceptance, and branching ratio of the decay channel, in addition to the overall number of events, have all been taken into account throughout the process of adjusting these distributions.[48] In addition to the data from inelastic pp collisions that took place at the same energy, the results of Pb-Pb collisions are published for eight distinct centrality classes, ranging from 0-10% all the way up to 70-80% in 10% broad centrality intervals. These findings are reported for eight different centrality classes. The p_T-integrated particle yields were obtained by the use of the approach that was provided. To match the p_T distributions, a Lévy-Tsallis function is employed in the pp, and a Boltzmann-Gibbs blast-wave function is utilized in the Pb-Pb collisions. Both of these functions are described below. It was feasible, with the assistance of fit functions, to extrapolate the yields into the unmeasured region with low and high p_T from the data from the region with the observed p_T. This was accomplished by taking the data from the region with the observed p_T. The application of low-p_T extrapolation includes the following: [49]

p_T<0.4 GeV/cfor K^{*0}(φ) When it comes to Pb–Pb collisions, it accounts for 12.5% (12.7%) of the total yield in the centrality class of 70–80% and 8.6% (7.2%) of the overall yield in the centrality class of 0–10%. It has been discovered that the K^{*0} in pp collisions may take on values between 0 and 1, with a value of 0 to p_T 20 GeV/c. The realm of applicability for the low-p_T extrapolation does encompass the meson. p_T 0.4 GeV/c, whic h is equivalent to 15.7% of the total output. When p_T is more than 20 GeV/c, the part of yield projected is almost zero.

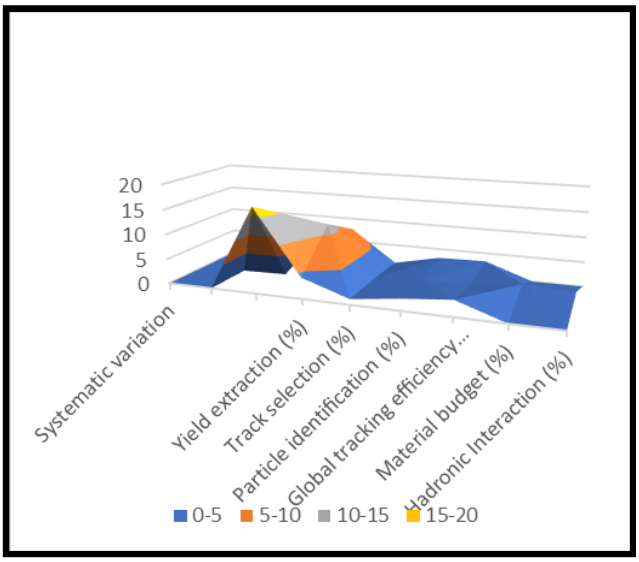

Fig. 2. the relationship between the ratios of the p_T-integrated particle yields K*^{0}/K* and K* $\langle dN_{ch}/d\eta \rangle^{1/3}$ collisions with energies of pp, p–Pb, and Pb–Pb exhibit evidence of midrapidity when measured. $\sqrt{s_{NN}}$ =5.02 TeV. For Pb–Pb collisions at $\sqrt{s_{NN}}$ =2.76 teraelectron volts, taking into account both the K*^{0}/K* and the K*^{0}/K^0 values. the relative frequency of particle p and particle Pb collisions. The systematic uncertainties for the total, charged-particle multiplicity-uncorrelated, and charged-particle multiplicity-correlated are depicted as boxes of various colors, in contrast to the statistical errors, which are shown as bars. Also included are the thermal model estimates for the most common Pb-Pb collisions. The chemical freeze-out temperature used in these calculations is T_{ch} = 156 MeV. Lines colored violet represent the predictions of the EPOS3 model for the K*^{0}/K* and K* ratios in Pb-Pb collisions.

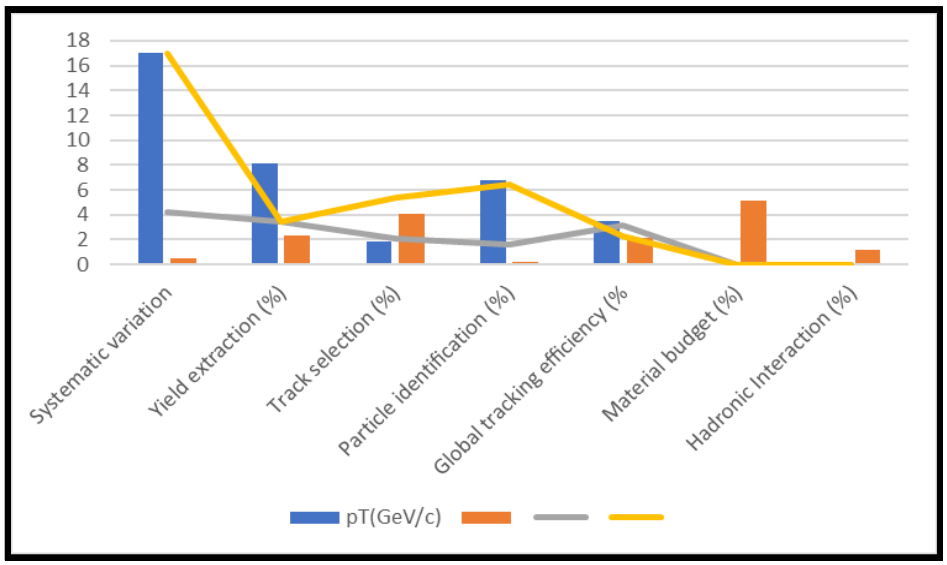

Fig. 3. A looser restriction on the duration of the hadronic phase based on the disparity between the chemical and kinetic freeze-outs $\langle dN_{ch}/d\eta \rangle^{1/3}$ collisions between p and Pb and Pb and Pb at $\sqrt{s_{NN}}$ =5.02 TeV. The bars and bands are representations of the statistical uncertainty and the systematic uncertainty, respectively, that have been propagated to the lifetime from the uncertainties associated with the observed K*^{0}/K* ratios in Pb–Pb (p–Pb) and pp collisions at different energies. This uncertainty was derived from the uncertainties associated with the measured K*^{0}/K* ratios in Pb–Pb (p–Pb) and pp collisions. $\sqrt{s_{NN}} = 5.02$ TeV.

Particle ratios

The K*^{0}/K* ratio and the /K* ratio are shown as a function of in Fig. 2. $\langle dN_{ch}/d\eta \rangle^{1/3}$ for Pb–Pb collisions at $\sqrt{s_{NN}} = 2.76$ and 5.02 TeV, p–Pb collisions at $\sqrt{s_{NN}} = 5.02$ TeV the kaon yields in Pb–Pb collisions at and pp collisions at $\sqrt{s_{NN}}$ =5.02 TeV. The $\langle dN_{ch}/d\eta \rangle^{1/3}$ This figure, which is determined based on the midrapidity measurement, will serve as a stand-in for the size of the system in this context. This notion has been given further weight thanks to the finding that the HBT radii increase in a linear fashion as the temperature rises. $\langle dN_{ch}/d\eta \rangle^{1/3}$ The K*^{0}/K* ratio gets lower as the value of K* goes up, but the /K* ratio is essentially unaffected by the value of K*. $\langle dN_{ch}/d\eta \rangle^{1/3}$. There appears to be a pattern that repeats itself throughout all of the different collision systems and collision energies that were looked into, and this pattern can be observed in the ratios. The ratios of K*^{0}/K* and /K* in particle–particle collisions involving lead–lead at different energies are as follows: $\sqrt{s_{NN}} = 2.76$ and 5.02 TeV are reliable even while the results are uncertain.

Regeneration and rescattering, which both lead to a decrease in the measured yields, affect the resonance yields during the hadronic phase. Regeneration can, however, also lead to an increase in the observed yields. The observed dependence of the K*^{0}/K* ratio on the charged-particle multiplicity is consistent with the behavior that was anticipated to exist in this circumstance if rescattering is the process that causes the suppression. The decay of the most likely occurs mostly outside of the hadronic medium since its lifetime is an order of magnitude longer than that of the K*^{0} and the K* ratio does not exhibit suppression with charged-particle multiplicity. This is because the lifespan of is a significant order of magnitude more than the lifetime of the K*^{0}.[50] This is caused by the fact that the lifespan of the K* is an order of magnitude larger than that of the K*^{0}. Theoretical simulations show that whereas 7% of K*^{0} mesons with p_T = 0 GeV/c decay within 5 fm/c after generation, 55% of K*^{0} mesons with p_T = 1 GeV/c decay within 5 fm/c (the typical estimate for the time between chemical and kinetic freeze-out in heavy-ion collisions). The time between chemical and kinetic freeze-out in heavy-ion collisions is often estimated to be this long. This calculation is based on the average length of time between the beginning of chemical and kinetic freeze-out during heavy-ion collisions.

Mesons that decay during that period with a p_T value of 1 GeV/c. This supports the theory that rescattering is responsible for the empirically observed decrease in the K*^{0}/K* ratio when the number of charged particles increases. Additionally, a similar type of suppression was seen for ρ0/π and Λ^*/Λ. When compared to peripheral Pb-Pb and pp collisions, core Pb-Pb collisions provide a greater amount of energy at high energies. $\sqrt{s_{NN}} = 2.76$ TeV. The calculated K*^{0}/K* ratio from thermal model calculations with no rescattering effects and with chemical freeze-out temperature T_{ch} = 156 MeV is also found to be higher than the corresponding measurements, while the measured K*ratio agrees with the predicted values for the most central Pb-Pb collisions. Although the computed K*^{0}/K* ratio is predicated on the presumption that there are no rescattering effects, it is discovered that this is the case. Even though the calculations were performed with T_{ch} = 156 MeV as the chemical freeze-out temperature, it was found that this is in fact the case. The K*^{0}/K* and K* ratios in Pb-Pb collisions are also compared to estimates obtained from the EPOS3 model. These comparisons are performed both with and without the UrQMD-specified hadronic cascade phase. Both versions of these comparisons—one with and one without a phase including a hadronic cascade—are performed. The picture displays the EPOS3 model's predictions for Pb-Pb collisions at various energies.

. $\sqrt{s_{NN}} = 2.76$ .TeV, but there should in no way, shape, or form be any identifiable qualitative differences between the two energies in any way, shape, or form. Reproduction by the EPOS3 generator, while utilizing UrQMD, of the trend of the K*^{0}/K* and K*ratios is more evidence that supports the results reached by the experiment.

CONCLUSION

In this experiment, the transverse momentum distributions of K^{*0} and mesons were observed when the particles were travelling at a speed that was on the slow side. (|y| <0.5) Pb-Pb and inelastic pp collisions have been studied, and numerous collision centralities have been found. $\sqrt{s_{NN}} = 5.02$ The ALICE detector is what enables TeV to be achieved. In contrast to collisions involving pp particles, Pb-Pb collisions result in a suppression of the K* yields for charged kaons. This suppression increases with the size of the system, which itself is a function of the size of the system. $\langle dN_{ch}/d\eta \rangle^{1/3}$ Using the midrapidity approach, try to compute. On the other hand, examining the mesons provides no proof that such suppression occurred. The extended life of the meson may be due to this lack of suppression. This is due to the fact that most mesons fragment outside of the fireball. $(\tau\varphi = 46.3 \pm 0.4\ fm/c)$ due to a reduced lifespan $(\tau K^{*0} = 4.16 \pm 0.05\ fm/c)$. K^{*0} decays are taking place in the hadronic medium, which is also where hadrons first appeared in significant quantities. Other hadrons that are present in the medium are able to interact with the decay product (or products), which results in a significant change in the momentum of those other hadrons. As a direct consequence of this, the K^{*0} signal's reconstruction in the experiment does not take into account the products of decay any more. The data that have been displayed here are an experimental demonstration of the predominance of rescattering effects in the hadronic phase of the system, which is produced by heavy-ion collisions. The facts reported here not only illustrate that rescattering and regeneration are possible in theory, but also that they may be verified empirically. The magnitude of the rescattering is inversely proportional to the size of the system. Even though the K^{*0}/K* yield ratios in center Pb-Pb collisions are substantially lower than the values from thermal model calculations without rescattering effects, the observed K* yield ratio coincides with the model calculation. This is because rescattering effects are not taken into account in the thermal model calculations. On the other hand, this kind of issue takes place when the K* yield ratio is considerably different from the results of the calculations that were carried out using the thermal model. The concept that rescattering has an effect on the K^{*0} yields found in Pb-Pb collisions receives more support as a result of this finding. A lower limit on the length of time that the hadronic phase lasts may be determined by using the K^{*0}/K* ratios that are produced in high-energy Pb-Pb and pp collisions.. $\sqrt{s_{NN}} = 5.02$ TeV. According to what one may reasonably assume, the lifetime improves in direct proportion to the size of the system. In the case of central Pb–Pb collisions, the value can range anywhere from 4 to 7 fm/c..

REFERENCES

[1] Adams, J.; Aggarwal, M.M.; Ahammed, Z.; Amonett, J.; Anderson, B.D.; Arkhipkin, D.; Averichev, G.S.; Badyal, S.K*.; Bai, Y.; Balewski, J.; et al. K*(892)* resonance production in Au + Au and p + p collisions at sNN−−−√SNN = 200 GeV at STAR. Phys. Rev. C 2005, 71, 064902.

[2] Adler, S.S.; Afanasiev, S.; Aidala, C.; Ajitanand, N.N.; Akiba, Y.; Alexander, J.; Amirikas, R.; Aphecetche, L.; Aronson, S.H.; Averbeck, R.; et al. Production of ϕ mesons at midrapidity in sNN−−−√ SNN = 200 GeV Au + Au collisions at relativistic energies. Phys. Rev. C 2005, 72, 014903.

[3] Abelev, B.; Aggarwal, M.M.; Ahammed, Z.; Amonett, J.; Anderson, B.D.; Anderson, M.; Arkhipkin, D.; Averichev, G.S.; Bai, Y.; Balewski, J.; et al. Strange Baryon Resonance Production in sNN−−−√ SNN = 200 GeV p + p and Au + Au collisions. Phys. Rev. Lett. 2006, 97, 132301.

[4] Abelev, B.; Adam, J.; Adamová, D.; Aggarwal, M.M.; Agnello, M.; Agostinelli, A.; Agrawal, N.; Ahammed, Z.; Ahmad, N.; Masoodi, A.A.; et al. [ALICE Collaboration] K**(892)0 and ϕ(1020) production in Pb-Pb collisions at sNN−−−√ SNN = 2.76 TeV. Phys. Rev. C 2015, 91, 024609.

[5] Adamová, D.; ALICE Collaboration; Aggarwal, M.M.; Rinella, G.A.; Agnello, M.; Agrawal, N.; Ahammed, Z.; Ahmad, S.; Ahn, S.U.; Aiola, S.; et al. Production of Σ(1385)± and Ξ(1530)0 in p-Pb collisions at sNN−−−√ SNN = 5.02 TeV. Eur. Phys. J. C 2017, 77, 389.

[6] Acharya, S.; Adamová, D.; Adolfsson, J.; Aggarwal, M.M.; Rinella, G.A.; Agnello, M.; Agrawal, N.; Ahammed, Z.; Ahn, S.U.; Aiola, S.; et al. Suppression of Λ(1520) resonance production in central Pb-Pb collisions at sNN−−−√ SNN = 2.76 TeV. Phys. Rev. C 2019, 99, 024905.

[7] Acharya, S.; Acosta, F.T.; Adamová, D.; Adolfsson, J.; Aggarwal, M.M.; Rinella, G.A.; Agnello, M.; Agrawal, N.; Ahammed, Z.; Ahn, S.U.; et al. Production of the ρ(770)0 meson in pp and Pb-Pb collisions at sNN−−−√ SNN = 2.76 TeV. Phys. Rev. C 2019, 99, 064901.

[8] Acharya, S.; Adamová, D.; Adler, A.; Adolfsson, J.; Aggarwal, M.; Rinella, G.A.; Agnello, M.; Agrawal, N.; Ahammed, Z.; Ahmad, S.; et al. Evidence of rescattering effect in Pb–Pb collisions at the LHC through production of K*(892)0∗ and ϕ(1020) mesons. Phys. Lett. B 2020, 802, 135225.

[9] Blaschke, D.; Aichelin, J.; Bratkovskaya, E.; Friese, V.; Gazdzicki, M.; Randrup, J.; Rogachevsky, O.; Teryaev, O.; Toneev, V. Topical issue on Exploring Strongly Interacting Matter at High Densities-NICA White Paper. Eur. Phys. J. A 2016, 52, 267.

[10] Particle Data Group; Zyla, P.A.; Barnett, R.M.; Beringer, J.; Dahl, O.; Dwyer, D.A.; Groom, D.E.; Lin, C.-J.; Lugovsky, K*.S.; Pianori, E.; et al. Review of Particle Physics. Prog. Theor. Exp. Phys. 2020, 2020, 083C01.

[11] Bass, S.A. Microscopic models for ultrarelativistic heavy ion collisions. Prog. Part. Nucl. Phys. 1998, 41, 255–369.

[12] Bratkovskaya, E.L.; Cassing, W.; Moreau, P.; Oliva, L.; Soloveva, O.E.; Song, T. PHSD—A Microscopic Transport Approach for Strongly Interacting Systems. arXiv Prepr. 2019, arXiv:1908.00451.

[13] Lin, Z.; K*o, C.M.; Li, B.-A.; Zhang, B.; Pal, S. Multiphase transport model for relativistic heavy ion collisions. Phys. Rev. C 2005, 72, 064901.

[14] Pierog, T.; K*arpenko, I.A.; K*atzy, J.M.; Yatsenko, E.; Werner, K*. EPOS LHC: Test of collective hadronization with data measured at the CERN Large Hadron Collider. Phys. Rev. C 2015, 92, 034906.

[15] Baznat, M.; Botvina, A.; Musulmanbekov, G.; Toneev, V.; Zhezher, V. Monte-Carlo Generator of Heavy Ion Collisions DCM-SMM. Phys. Part. Nucl. Lett. 2020, 17, 303–324.

[16] Vislavicius, V.; K*alweit, A. Multiplicity dependence of light flavour hadron production at LHC energies in the strangeness canonical suppression picture. arXiv Prepr. 2016, arXiv:1610.03001.

[17] ALICE Collaboration. Enhanced production of multi-strange hadrons in high-multiplicity proton–proton collisions. Nat. Phys. 2017, 13, 535–539.

[18] F. Becattini, G. Passaleva, Eur. Phys. J. C 23, 551 (2002).

[19] F. Becattini, P. Castorina, J. Manninen, H. Satz, Eur. Phys. J. C 56, 493 (2008)

[20] Andronic, F. Beutler, P. Braun-Munzinger, K*. Redlich,

[21] J. Stachel, Phys. Lett. B 675, 312 (2009).

[22] Andronic, P. Braun-Munzinger, J. Stachel, Nucl. Phys. A 772, 167 (2006).

[23] K*raus, J. Cleymans, H. Oeschler, K*. Redlich, S. Whea- ton, Phys. Rev. C 76, 064903 (2007).

[24] Cleymans, B. K*¨ampfer, P. Steinberg, S. Wheaton, J. Phys. G 30, S595 (2004).

[25] B. K*¨ampfer, J. Cleymans, P. Steinberg, S. Wheaton, Heavy Ion Phys. 21, 207 (2004).

[26] Cleymans, B. K*ampfer, M. K*aneta, S. Wheaton, N. Xu, Phys. Rev. C 71, 054901 (2005).

[27] HADES Collaboration (G. Agakishiev et al.), Eur. Phys. J. A 47, 21 (2011).

[28] J. Steinheimer, M. Bleicher, J. Phys. G 43, 1, 015104 (2016).

[29] S. Wheaton, J. Cleymans, Comput. Phys. Commun. 180, 84 (2009). Particle Data Group (K*. Hagiwara et al.), Phys. Rev. D 66, 010001 (2002).

[30] Particle Data Group Collaboration (K*.A. Olive et al.), Chin. Phys. C 38, 090001 (2014)

[31] HADES Collaboration (G. Agakishiev *et al.*), Eur. Phys. J. A 41, 243 (2009).

[32] HADES Collaboration (M. Lorenz *et al.*), PoS (BORMIO2010) , 038 (2010).

[33] FOPI Collaboration (K*. Piasecki *et al.*), Phys. Rev. C 91, 054904 (2015).

[34] FOPI Collaboration (P. Gasik *et al.*), arXiv:1512.06988 [nucl-ex].

[35] N. Herrmann, J.P. Wessels, T. Wienold, Annu. Rev. Nucl. Part. Sci. 49, 581 (1999).

[36] W. Reisdorf, H.G. Ritter, Annu. Rev. Nucl. Part. Sci. 47, 663 (1997).

[37] FOPI Collaboration (W. Reisdorf *et al.*), Nucl. Phys. A 848, 366 (2010).

[38] S.A. Bass *et al.*, Prog. Part. Nucl. Phys. 41, 225 (1998).

[39] HADES Collaboration (H. Schuldes *et al.*), J. Phys. Conf. Ser. 599, 012028 (2015).

[40] HADES Collaboration (P. Tlusty *et al.*), arXiv:0906.2309 (2009).

[41] HADES Collaboration (G. Agakishiev *et al.*), Phys. Rev. C 80, 025209 (2009).
[42] Aamodt K* et al. (ALICE Collaboration) 2011 Strange particle production in proton-proton collisions at √ s=0.9 TeV with ALICE at the LHC Eur. Phys. J. C 71 1594
[43] Aamodt K* et al. (ALICE Collaboration) 2011 Production of pions, kaons and protons in pp collisions at √ s=900 GeV with ALICE at the LHC Eur. Phys. J. C 71 1655
[44] Abelev B et al. (STAR Collaboration) 2012 Multi-strange baryon production in pp collisions at √ s=7 TeV with ALICE Phys. Lett. B 712 309
[45] Abelev B et al. (STAR Collaboration) 2006 Strange baryon resonance production in √ sNN=200 GeV p+p and Au+Au collisions Phys. Rev. Lett. 97 132301
[46] Abelev B et al. (STAR Collaboration) 2009 Systematic measurements of identified particle spectra in pp, d+Au, and Au+Au collisions at the STAR detector Phys. Rev. C 79 034909
[47] M. Bleicher et al. J. Phys. G25 (1999) 1859-1869
[48] S. Acharya et al. (ALICE Collaboration), Phys. Rev. C99 024905
[49] [(STAR Collaboration) https://doi.org/10.48550/arXiv.2210.02909
[50] S. Acharya et al. (ALICE Collaboration), Phys. Rev. C102 024912